A Cutting-Edge Bio-Inspired Computational Framework for **Advanced Virtual Reality Classification through Sophisticated Predictive Methodologies**

Yanyan Song, Hongping Zhou*

¹ School of Communication Technology, Communication University of China Nanjing, Nanjing 211172, China

*Corresponding Author

E-mail: zhouhongping1231@163.com

Keywords: virtual reality, histogram gradient boosting classification, decision tree classification, ebola optimization search, differential squirrel search algorithm

Received: May 20, 2025

Virtual reality (VR) enables the simulation of a wide variety of complex environments, from tiny biological structures to entirely imaginary worlds. These simulations create new possibilities for learning, training, and interaction that go beyond the limits of the physical world. However, virtual reality (VR) realizes this imaginary world, so it is not just a dream. VR works through the invocation of many of the senses. It creates realistic simulations through the creation of immersive settings that combine the real and the imagined, thereby affording special hands-on learning possibilities in a variety of subjects. This study investigates the effectiveness of combining Histogram Gradient Boosting Classification (HGBC) with Decision Tree Classification (DTC), the Ebola Optimization Search (EOS), and the Differential Squirrel Search Algorithm (DSSA) to predict VR outcomes. By integrating these advanced predictive and optimization techniques, the approach aims to enhance accuracy. Research will be conducted to ascertain the possible uses of VR, enhance user experience, and assess the impact on industries related to training, education, healthcare, and entertainment. In the evaluation phase, HGDS attained the highest accuracy of 0.967 in the test phase, making it the top-performing hybrid model, while DTEO showed the lowest accuracy of 0.907, identifying it as the weakest model.

Povzetek: Članek predstavi bio-navdihnjen hibridni okvir za klasifikacijo uporabniških odzivov v virtualni resničnosti. Združuje HGBC, DTC ter optimizatorja EOS in DSSA za izboljšanje napovedne točnosti. Okvirjeva naloga je zanesljivo razvrščati VR-podatke.

Introduction

VR simulation signifies a computer-created environment where users can move around, interact with objects, and interact with virtual characters, also implied as "agents" or "avatars." A generic virtual setting is a 3D world [1], and, like gravitation simulation, virtual environments frequently aim to be as realistic as possible in both appearance and object behavior. It must be underlined, nonetheless, that there need to be no parallels between this virtual environment and the actual world. One of the advantages of virtual environments is their ability to replicate completely unrealistic scenarios [2]. Virtual environments, however, provide a safe space to test scenarios that would be too dangerous or difficult to perform in real life, and they imitate the setting where the student will eventually work.

There are other ways of deploying VR; four typical configurations are included below:

- ✓ Desktop VR (Monoscopic or Stereoscopic)
- ✓ Immersive VR (HMD, CAVE, widescreen)
- Collaborative Systems
- Mixed or Augmented Reality

The desktop VR enables the user to interact with the system using a mouse or other controlling device while sitting in front of a desktop computer monitor, as the name implies [3]. Immersion systems utilize a visualization display worn on the head of the user that completely occludes their field of view. Collaborative systems have human-controlled avatars interacting with each other, and they can be immersive or desktop-based systems. Second Life is one of the most recent and most effective collaboration systems [4]. An attempt is also being made to use the collaborative systems for exploration. The mixed reality systems merge computer-generated matter with the real environment, which is viewed directly or through a camera. This system can teach engineering and medical skills to students, which are thought to be impossible by this recently invented system [5].

Learning by humans requires interaction with the environment, taking in information provided by the use of senses and experience [6]. Through computer simulation, VR takes the role of real-world sensory input. Reacting to motion and common human behaviors in the actual world offers interaction. Therefore, VR can be useful in education since it allows pupils to experience a situation

or scenario firsthand rather than only imagining it [7]. The three main components that define the quality of VR experiences are immersion, interaction, and multisensory feedback. Immersion is being engulfed or enclosed by the surroundings [8]. One of the advantages of immersion is that it ensures a feeling of presence or the perception that one is actually in the world being displayed [9]. Interactivity means the capability of the user's body movements to affect the events happening in the simulation and, in turn, provoke a reaction from the simulation [10], [11].

The multisensory nature of VR allows information to be derived from several senses, which further enhances the experience in that this makes it both more engaging and more convincing—increasing, as it does, the sensation of presence because this provides redundancy information, which diminishes the likelihood of misunderstanding. Information from multiple sensory entries is reinforced by a sensory combination [12], [13]. VR enables the user to act as though they are in the actual world by substituting a virtual environment for the current one. A constructivist learning approach benefits from VR's immersive features [14]. The premise of constructivism, a theory of knowledge acquisition, is that people build knowledge by concluding from their past experiences. The idea, as propounded by Jean Piaget, assumes that learners try to fit new experiences into the world picture that they have developed earlier. Learners change their worldview to fit the new experience when they cannot assimilate new information into their system effectively. Learning comes from experiences where actions are based on assumptions about how the world functions, only to find that it does not align with those assumptions [15], [16], [17]. Adjusting the mental model of how the world functions becomes necessary to account for the new experience. The view is that learning is an active process of testing hypotheses. In other words, this concept contrasts with the notion of learning as something passive in nature: the mere acquisition or assimilation of data. VR is a powerful learning tool because it provides a context where such hypothesis testing can occur. According to [18], students who interact with new material are more likely to store and recall it.

Control software is at the heart of this system. This regulates the exchange of information between the virtual world and the interface layer in response to user actions, updating the world appropriately. On display devices such as the haptic and visual interface, it also determines when the scene should be shown. With the help of additional tools, the control software can connect to the outside world through the internet, which might be an essential capability in systems involving collaboration or many users. The virtual environment module includes a model of real-world entities and the virtual world model. It includes state and position information apart from appearance. They could be dynamic objects, such as moving objects or even avatars. They could also be static objects. This model of the virtual environment needs to be refreshed at regular intervals to add dynamic objects [19]. The module for the virtual environment, which would store positions, shapes, and other attributes of all components of the virtual world in a database, is called the virtual environment module. The physics engine is one of the major parts of any realistic simulation. A physics engine comprises a set of rules that control the motion and interaction of dynamic objects in a virtual scene. A typical physics engine can include a Newtonian mechanics simulation and collision detection, which describes when two objects collide. They apply gravitational, friction, and impulse effects using physical rules. When two things hit each other, the latter effect is important [20], [21]. When two active entities collide, collision detection is necessary. The physics engine determines their terminal velocity using their simulated traits, such as mass, substance, and speed.

1.1 Related works

Normally, state-of-the-art reports that focus on specific aspects of the discipline or on specific application fields are available. They would mostly provide the taxonomies that systematically illustrate and classify the various methodologies involved.

- ➤ While Dachselt and Hübner [22] examined the menus for AR and VR environments for all of the MR domain [23], they also presented an extensive taxonomy.
- A taxonomy of NVEs, taking into consideration distribution and communication topologies, has been provided by Macedonia and Zyda [24]. Mania and Chalmers [25] have presented a taxonomy of platforms and communication.
- Bowman has provided several taxonomies for both interaction methods [26] and navigation methods [27]. Mine's early research [28] identifies the essential navigation and interaction in virtual spaces.
- ➤ Gabbard [29] provides good generalized overviews, presents suggested best practices in application design, and provides guides for conducting user evaluations. Livatino and Koeffel have also presented guidelines for Virtual Environments (VEs) assessment [30].
- ➤ The current tracking technology is overviewed by Welch and Foxlin [31], who also compare and contrast the respective merits and disadvantages of each.

Recent work has explored innovative methods for classifying virtual reality (VR) using bio-inspired computational models. Song and DiPaola [32] introduced a bio-responsive VR system based on physiological data to enhance immersion. Zayed and Reda [33] demonstrated that applying neurophysiological biosignals combined with deep learning could classify cognitive states in VR with 97% accuracy. Similarly, Arslan et al. [34], [35], [36], [37], [38] employed emotion classification from biosignals and machine learning in VR, achieving 97.78% accuracy. These advancements are significant in areas such as rehabilitation, education, and psychotherapy. VanHorn and Çobanoğlu [35] also developed a biomedical image classification system within a VR-based environment, making AI more accessible to experts.

Overall, these studies emphasize how biosignals, machine learning, and VR can be integrated to develop advanced predictive models, showcasing the potential of bioinspired computational models to improve classification techniques.

1.2 The study's objective

This work examines the possible contribution that VR technology will make to enhance learning outcomes and increase student engagement in schools. In data classification, this study applies an HGBC model and a DTC model. The performance of the schemes is optimized by using methods such as EOS and DSSA. This research will explore the integration of VR within diverse disciplines of study to understand how it can facilitate the retention of both theoretical knowledge and practical competencies of learners, given the immersion one experiences in a VR environment. Possible drawbacks and limitations, including accessibility of resources, shall also be discussed to present a comprehensive overview of what can be expected from this educational technology.

2 Materials and methodology

2.1 **Data gathering**

A set of users' experiences in VR settings provides the dataset. The information covers user preferences, emotional moods, and physiological reactions like skin conductance and heart rate. This study's dataset includes 1000 samples, each representing a user's VR session. Recorded features encompass User ID (173 unique values), Age (66), Gender (147), VR Headset type (61), Session Duration (137), Motion Sickness severity (56), and Immersion Level (55). These variables cover both demographic and behavioral data. forming comprehensive basis for analysis. The Immersion Level serves as the target variable, indicating users' subjective

ImmersionLevel 3,500 2.6 3.000 2.4 2,500 2.0 1.8 1.6 1.000 1.4

engagement in VR, and its variability supports the creation of effective predictive models.

This dataset attempts to contribute to the development of VR through the analysis of user experiences. An attempt has been made in this study to develop a better VR design with much more improvement in user comfort and customization by understanding the physical emotional reactions of consumers in diverse situations. This information allows developers to work on boosting VR systems and creating personalized experiences that will enhance customers' delight and immersion. Fig. 1 presents a contour plot for the correlation of the features.

User ID: This variable identifies every participant who experienced VR. Each user is assigned a unique ID so that their data in the dataset can be differentiated.

Age: This variable stores the age of the subject participating in VR exposure. For example, this could be an integer representing the current user's age at the time of using the VR.

Gender: This variable displays the user's gender. The categories "Male," "Female," and "Other" can be utilized to define the user's gender identity.

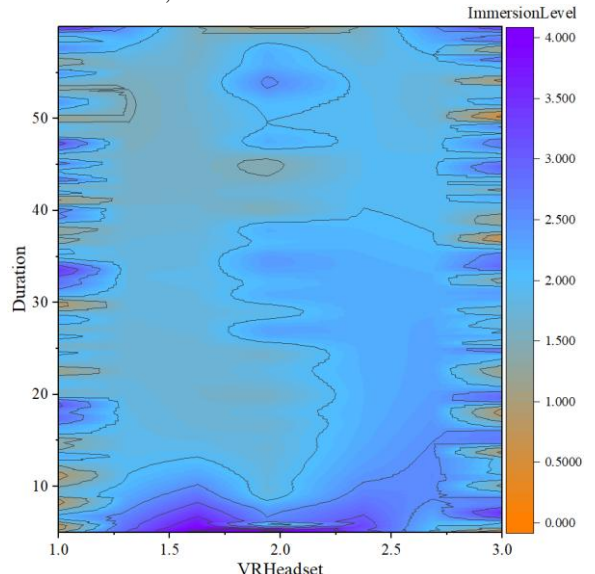
VR Headset Type: This would be a variable specifying the form of VR headset that a user is utilizing in a VR experience. Examples include Oculus Rift, HTC Vive, and PlayStation VR, among others.

Duration: This variable shows the time spent in the VR experience in minutes. It reflects how much time was spent by the participant in the VR setup.

Motion Sickness Rating: It displays the rating of the user's self-reported motion sickness during the VR experience. Higher numbers relate to a higher degree of motion sickness on an ascending scale ranging between 1 and 10.

Dependent variable:

The degree to which a user experiences being inside a virtual environment quantifies the subjective degree of the user's feeling of immersion in the experience, with a rating between 1 and 5, where 5 stands for the maximum level.



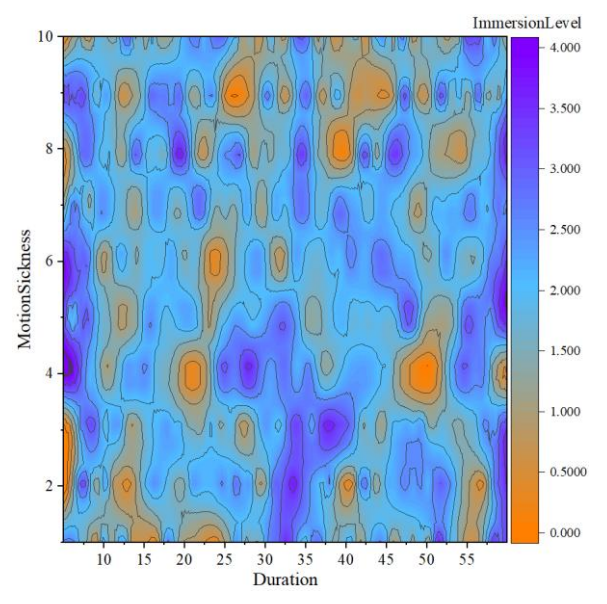


Figure 1: The contour plot with color fill illustrates the relationship between input and output variables

Before deploying advanced computational models, understanding several challenges in VR classification systems is essential. These encompass the significant variability in user responses driven by individual physiological and psychological differences, noise in biometric data such as heart rate and skin conductance, and class imbalance across different immersion levels. The subjective nature of immersion also complicates labeling and impacts the consistency of ground truth. These factors result in a complex, high-dimensional feature space where traditional classifiers often face difficulties with generalization and robustness. Consequently, adopting adaptive hybrid machine learning approaches, supported by powerful metaheuristic optimization techniques, is crucial for effective classification in VR.

2.2 Histogram gradient boosting classification (HGBC)

The HGB approach is another variant of the popular GB [39] technique used to resolve diverse classification and regression-oriented machine learning (ML) problems. These schemes, which AdaBoost also belongs to, primarily try to turn weak learners into strong ones. They come under the category of schemes called boosting schemes. Boosting techniques try to keep adding and teaching new weak learners successively to correct their previously introduced weak learners about their mistakes. It then informs each new weak learner to avoid the mistakes made by its forerunner. The most common weak learners used are DTs. This resulted in the development of the HGB algorithm, a boosting methodology that overcame one of the major weaknesses of the GB algorithm, which was its very long training time when training on large datasets. To circumvent this problem, the continuous input variables are discretized or binned into a few hundred distinct values. In this case, the learning rate (LR) of the scheme is the most important hyperparameter. Much attention was paid to the optimization of the scheme through several iterations of hyperparameter tweaking. The implementation of HGB from sci-kit-learn 0.21.3 was used from the Python ML module [40].

2.3 Decision tree classification (DTC)

In a DT, every internal node displays a characteristic, each branch is a decision rule, and each leaf node is the outcome [41]. The root node signifies the topmost node in a DT. To achieve the best discrimination among classes or results, it learns to split based on the value of an attribute. Different schemes have different criteria regarding making decisions. For example, some of the metrics used by schemes like ID3, C4.5, and CART include entropy, gain ratio, and Gini impurity, respectively. The problem at hand now is to find that characteristic at every level that offers the optimum split in a DT, thereby assisting optimum decision-making [42]. The concept can be mathematically understood by using the DT split based on entropy. The entropy H(D) of a dataset D can be calculated as follows:

$$H(D) = -\sum_{i=1}^{m} p_i log_2 p_i \tag{1}$$

2.4 Ebola optimization search (EOS)

Driven by the diffusion of the Ebola virus, in what follows, EOS presents a metaheuristic scheme [43]. The EOSA scheme is based on the enhanced SIR scheme of the sickness. Its S, E, I, R, H, V, Q, and D compartments represent the Susceptible (S), Exposed (E), Infected (I), Hospitalized (H), Recovered (R), Vaccinated (V), Quarantine (Q), and Death (D) states, respectively. Because of these compartments, the composition provides for the construction of a search domain that best displays combinations of weights and biases that may be required by CNN. After representation, SIR is displayed by a mathematical scheme utilizing a system of first-order differential equations. Then, the new metaheuristic scheme was developed by combining the mathematical

and propagation schemes, and later, the obtained mathematical scheme was deployed in the design of EOSA-CNN for experimentation. Therefore, the following are the mathematical schemes:

$$mI_i^{t+1} = mI_i^t + \rho M(I) \tag{2}$$

$$\frac{\partial S(t)}{\partial t} = \pi - (\beta_1 I + \beta_3 D + \beta_4 R + \beta_2 (PE)\eta)S - (\tau S + \Gamma I)$$
(3)

$$-(\tau S + \Gamma I)$$

$$\frac{\partial I(t)}{\partial t} = (\beta_1 I + \beta_3 D + \beta_4 R + \beta_2 (PE)\lambda)S$$

$$-(\Gamma + \gamma)I - (\tau)S$$
(4)

$$\frac{\partial H(t)}{\partial t} = \alpha I - (\gamma + \varpi)H \tag{5}$$

$$\frac{\partial \ddot{R}(t)}{\partial t} = \gamma I - \Gamma R \tag{6}$$

$$\frac{\partial V(t)}{\partial t} = \gamma I - (\mu + \vartheta)V \tag{7}$$

$$\frac{\partial D(t)}{\partial t} = (\tau S + \Gamma I) - \delta D \tag{8}$$

$$\frac{\partial \dot{D}(t)}{\partial t} = (\tau S + \Gamma I) - \delta D \tag{8}$$

$$\frac{\partial \ddot{Q}(t)}{\partial t} = (\pi I - (\gamma R + \Gamma D)) - \xi Q \tag{9}$$

 $\frac{\partial Q(t)}{\partial t} = (\tau S + \Gamma I) - o\nu$ $\frac{\partial Q(t)}{\partial t} = (\pi I - (\gamma R + \Gamma D)) - \xi Q \qquad (9)$ $mI_i^{t+1} \text{ and } mI_i^t \text{ display the old and new situation at}$ time t and t + 1, respectively, ρ is the displacement scale factor of an individual in Eq. (2). The data updated here are Hospitalized (H), Vaccinated (V), Recovered (R), Infected (I), Susceptible (S), Quarantine (Q), and Dead (D). Eqs. (3) to (9) define a system of ordinary differential equations, all of the scalar functions that one can evaluate to float values. These are computed given initial conditions $S(0) = S_0, I(0) = I_0, R(0) = R_0, D(0) =$ D_0 , $P(0) = P_0$, and $Q(0) = Q_0$, t is after the definition of iterations. This will then enable us to conclude the magnitude of vectors S, I, H, R, V, D, and Q at t.

The pseudocode that describes the EOSA metaheuristic scheme is presented accordingly in steps below:

- Define initial values for all vector and scalar quantities, that is, persons and parameters, respectively: the numbers of hospitalized (H), vaccinated (V), susceptible (S), infected (I), recovered (R), dead (D), and quarantined (Q).
- I_1 is created at random among vulnerable people.
- The value of fitness shall be calculated at the index case, having set that as the current and global best.
- If there is at least one infected person and the number of iterations is not reached, then:
- With every vulnerable individual, a standing is created and altered accordingly with their movement. Exploitation is characterized by short displacement; otherwise, it characterizes exploration. Remember that the longer an infected case is displaced, the more infections there are.
- b) Using (a), generate newly infected individuals nI.
- Create the new individuals and add the new instances in *I*.
- From the size of I calculate how many people are added to H, D, R, B, V, and Q at their respective rates.
- Utilizing the new I, refine S and I. e)
- Compare the best I have got at the moment with the best in the world.
- If the termination condition is not reached, go back to step 4.
- Return all solutions and the best global resolution.

The design and discussion of the utilization of the enhancement issue defined in this paper are given in the following subsections.

Fig. 2 presents the flowchart of the DTC.

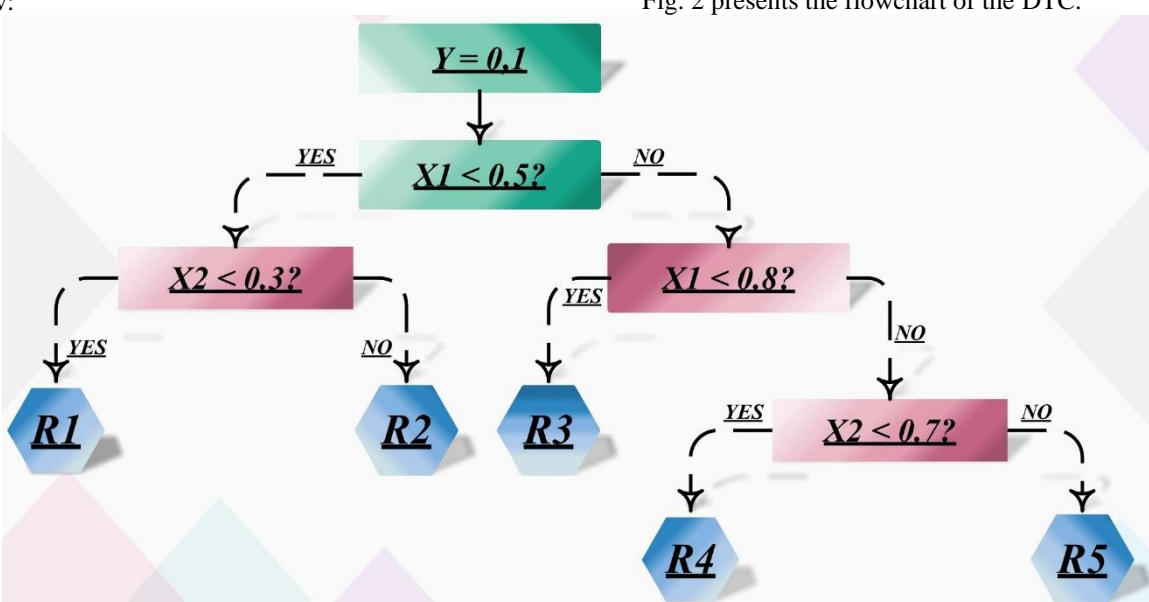


Figure 2: The flowchart of the DTC model

2.5 Differential squirrel search algorithm (DSSA)

DSSA, a hybrid optimizer that combines the differential evolution and squirrel search schemes is presented in this section. In SSA, the squirrels maintain the position of other squirrels regarding acorn or hickory trees for updating their position. To improve its search strategy, the top squirrels' position updating rules have been changed. The incorporation of crossover operations inspired by DE significantly enhances the exploration capability.

The following is a mathematical scheme of many foraging techniques covered under the paradigm of DSSA.

To justify selecting EOS and DSSA for this classification task, it's crucial to highlight the problem's nature: the dataset involves multiple interacting features with complex, nonlinear relationships, which can cause optimization to get stuck in local optima when using traditional methods. The EOS algorithm, inspired by epidemic modeling, employs dynamic, population-based exploration techniques that balance infection-driven diversification with recovery-focused convergence. This strategy is especially effective for tuning hyperparameters in complex models like HGBC and DTC. Its compartmental diffusion model efficiently captures multidimensional search dynamics. Meanwhile, DSSA mimics squirrel foraging behavior and utilizes crossover inspired by differential evolution, making it highly effective at fine-tuning solutions locally maintaining overall diversity. This capability is critical in VR classification scenarios, where high accuracy requires careful adjustment of sensitive parameters to prevent overfitting. DSSA's ability to retain elite solutions while

fostering diversity helps avoid premature convergence.
$$PS_{at}^{new} = \begin{cases} PS_{at}^{old} + d_g \times G_c (PS_{ht}^{old} - PS_{at}^{old} - P_{avg}), & r_1 \ge P_{dp} \\ random \ position, & otherwise \end{cases}$$

whereas P_{avg} is the mean location of every squirrel in the current population.

It also employs the crossover mechanism of DE in a way that ensures diversity among squirrels to the maximum while minimizing the possibility of trapping in local minima. Applied to the squirrel's current position and the new position as obtained by Eq. (11):

$$PS_{at,i,j}^{cr} = \begin{cases} PS_{at,i,j}^{new}, & if(rand_j \leq Cr) \text{ or } j = j_{rand} \\ PS_{at,i,j}^{old}, & if(rand_j > Cr) \text{ or } j \neq j_{rand} \end{cases}, j$$

$$= 1, 2, 3, ..., D$$
(11)

In this context, NP displays the population size, with i ranging from 1, 2, 3, ..., NP. For acorn or normal trees, $PS_{at;i;j}^{cr}$ indicates the updated positions of the squirrels following the crossover operation. $PS_{at;i;j}^{new}$ and $PS_{at;i;j}^{old}$ correspond to the new and previous positions of the squirrels. D refers to the dimensionality of the problem, and Cr displays the crossover rate, which is set to 0.5. The index j_{rand} is randomly selected from the range [1, D], and $rand_j$ denotes the jth random number, uniformly generated within this range.

Combining EOS and DSSA offers complementary advantages, EOS facilitates broad exploration, while DSSA ensures precise convergence, together enhancing classification accuracy and model robustness for VR immersion prediction.

2.5.1 Initialization of position and evaluation of fitness

The squirrels are initially placed in the search area at random. Knowing the squirrels' location allows one to calculate their fitness, which simply replaces their position in the fitness function by demonstrating how good a food supply they could find. The best squirrel PS_{ht} discovered in the hickory tree thus far is determined by sorting fitness values. It is thought that the squirrels in the acorn tree $PS_{at}(1:3)$ are traveling in the direction of the optimal location in a subsequent iteration, as indicated by the following three best function values. The remaining squirrels, $PS_{nt}(1:NP-4)$, are in the typical tree and have not yet discovered food.

2.5.2 Position update

The squirrels in an acorn tree, following the current best, PS_{ht} , renew the position, and move in the direction of the best source when there is no predator. The squirrels of a usual tree follow the ones in an acorn or hickory tree to renew their position. If there is the presence of a predator, then the squirrels change direction randomly while foraging. These are the mathematical schemes that are used to update the squirrel's position.

As in Eq. (10) now, the posture of squirrels on acorn trees changes based on the postures of others.

$$\geq P_{dp}$$
 (10)

Some of the squirrels on regular trees do the placement of acorn tree squirrels, after which they relocate to their new locations.

$$= \begin{cases} PS_{nt}^{old} + d_g \times G_c(PS_{at}^{old} - PS_{nt}^{old}), r_2 \ge P_{dp} \\ random \ position, \quad otherwise \end{cases}$$
 (12)

where the random integer r_2 is uniformly distributed between 0 and 1.

In normal trees, the survivors cling on to the best move on view, and their new positions are shown below: PS_{nt}^{new}

$$= \begin{cases} PS_{nt}^{old} + d_g \times G_c (PS_{ht}^{old} - PS_{nt}^{old}), r_3 \ge P_{dp} \\ random \ position, \quad otherwise \end{cases}$$
 (13)

The following crossover procedure is also given for typical tree squirrels:

$$= \begin{cases} \frac{PS_{nt,i,j}}{PS_{nt,i,j}}, & if(rand_j \leq Cr)or \ j = j_{rand} \\ \frac{PS_{nt,i,j}^{old}}{PS_{nt,i,j}^{old}}, & if(rand_j > Cr)or \ j \neq j_{rand} \end{cases},$$

$$j = 1, 2, 3, ..., D$$

$$(14)$$

The convergence speed may be raised by permitting the hickory tree squirrel to update her location in relation

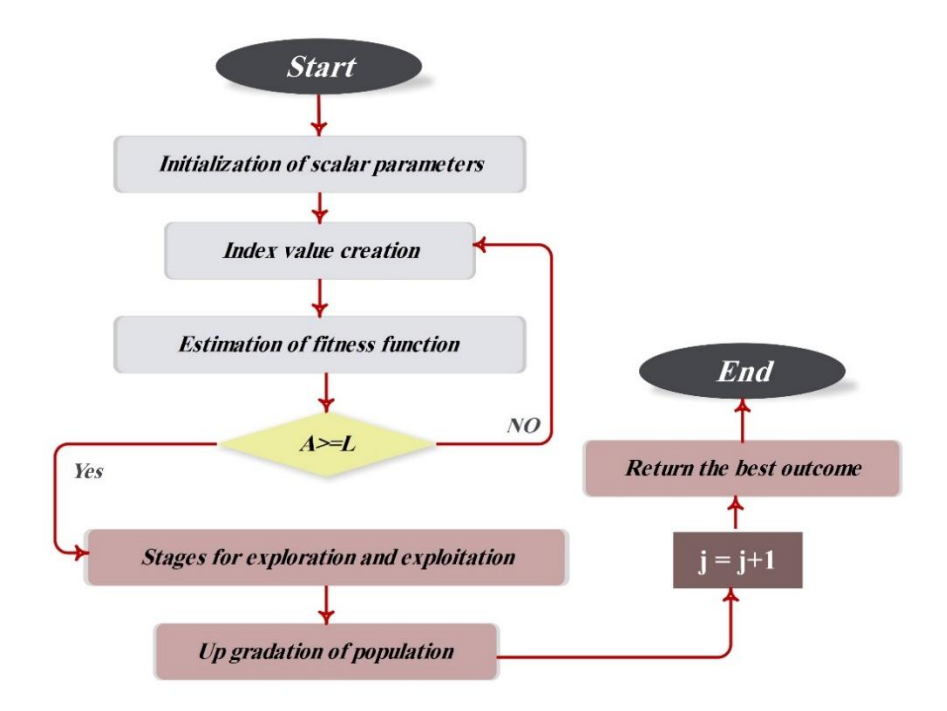
to the average position of the squirrels in the tree. This can be done as follows:

$$PS_{ht}^{new} = PS_{ht}^{old} + d_g \times G_c(PS_{ht}^{old} - PS_{at}^{avg})$$
 (15)

In this instance, PS_{avg} displays the average of all squirrel locations within the acorn trees.

In order to participate in the next generation of people, the best aspects of the new work, as well as its crossover roles, are then contrasted with the old jobs.

Figure 3 illustrates the flowchart of the proposed hybrid models (such as HGDS and DTEO), detailing the sequential phases that encompass data input, model development, optimizer-centric hyperparameter optimization, training, and final assessment. This diagram delineates the interaction between machine learning models and metaheuristic optimizers within the hybrid structure.



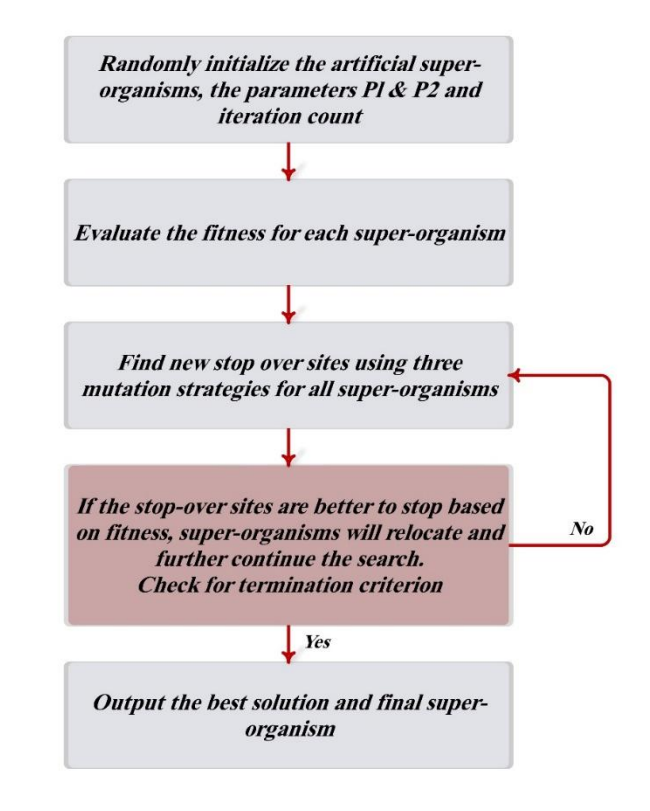


Figure 3: The process flowchart of the proposed hybrid models

2.6 Performance evaluators

Accuracy depends on how many correctly projected positive and negative instances there are of the total, defined by True Positives (TP), True Negatives (TN)correctly projected negative cases, False Positives (FP)incorrectly projected as positive, and False Negatives (FN)—incorrectly projected as negative. Using TP and FP as the relevant measures, precision gauges the percentage of TP projections out of all the positive projections the model has made. Smaller amounts of false positives imply higher precision. Recall is the measure of the share of TP projections from all real positive instances, using True Positives and False Negatives; it indicates that the model will detect all relevant positive cases. The fewer false negatives there are, the higher the recall. A simple statistic that balances the trade-off between Precision and Recall is the F1 score. It combines the two.

$$Accuracy: \frac{TP + TN}{TP + FP + FN + TN} \tag{16}$$

$$Precision: \frac{TP}{TP + FP} \tag{17}$$

$$Recall: \frac{TF}{TD + FN} \tag{18}$$

$$F1 - score = 2 \times \frac{Precision \times Recall}{Precision + Recall}$$
 (19)

The F1-score is a single measure that balances the accuracy and recall; it is the harmonic mean of both. It is very useful when considering false negatives and false positives. The greater the F1 score, the better balanced the recall and accuracy.

3 Results and discussion

3.1 Hyperparameters tuning and convergence curve analysis

The presented table displays the tuned hyperparameters for four different hybrid models: HGEO, HGDS, DTEO, and DTDS. Seven key hyperparameters were considered to optimize these models' performance: learning_rate, max_leaf_nodes, max_depth, min_samples_leaf, max_bins, min_samples_split, and a second instance of

max_leaf_nodes (listed separately for different model types). The HGEO and HGDS models, based on the HGBR algorithm, have specified values for learning_rate, max_leaf_nodes, max_depth, min_samples_leaf, and max_bins. For example, the HGEO model has a learning rate of 0.709, max leaf nodes of 278, max_depth of 100, min_samples_leaf of 10, and max_bins of 27. In the HGDS model, these values are learning_rate of 0.148, max_leaf_nodes of 557, max_depth of 893, min_samples_leaf of 7, and max_bins of 102. Conversely, the DTEO and DTDS models, which are based on decision tree algorithms, do not include values for learning rate, max leaf nodes, or max bins in the first part of the table. However, they include defined values for max_depth, min samples leaf, min samples split, max leaf nodes in the second part. For instance, the DTEO model has max depth of 741, min samples leaf of 0.00025. min_samples_split of 0.0275. max_leaf_nodes of 2710. Similarly, the DTDS model features max_depth of 597, min_samples_leaf of 0.00025, min_samples_split of 0.0005, and max_leaf_nodes of 1789. Overall, the table indicates that hyperparameters are selectively tuned for each model based on its structure, with parameter values chosen according to each model's specific characteristics and requirements.

Fig. 4 displays a 3D waterfall plot illustrating the convergence curves of four hybrid schemes: HGDS, HGEO, DTDS, and DTEO. The plot effectively visualizes the different convergence rates and final performance levels of the schemes, demonstrating the varying degrees of effectiveness in the optimization process. This comparison emphasizes the significance of the number of iterations and initial accuracy in determining the overall success of each hybrid model. The HGDS model starts with an accuracy of 0.6 and gradually improves over 200 iterations, ultimately reaching a peak accuracy of 0.967, making it the highest-performing model among the four. The other three schemes begin with a lower accuracy of 0.4 and converge more quickly than HGDS, reaching their final accuracy in fewer iterations. Among these schemes, DTEO is identified as the weakest hybrid model, with a final accuracy of 0.908 after its iterations.

Table 1: Hyperparameter tuning for four models

Hun ann an ann at ans	Models				
Hyperparameters	<i>HGEO</i>	HGDS	DTEO	DTDS	
learning_rate	0.709	0.148	-	-	
max_leaf_nodes	278	557	-	-	
max_depth	100	893	741	597	
min_samples_leaf	10	7	0.00025	0.00025	
max_bins	27	102	-	-	
min_samples_split	-	-	0.0275	0.0005	
max_leaf_nodes	-	-	2710	1789	

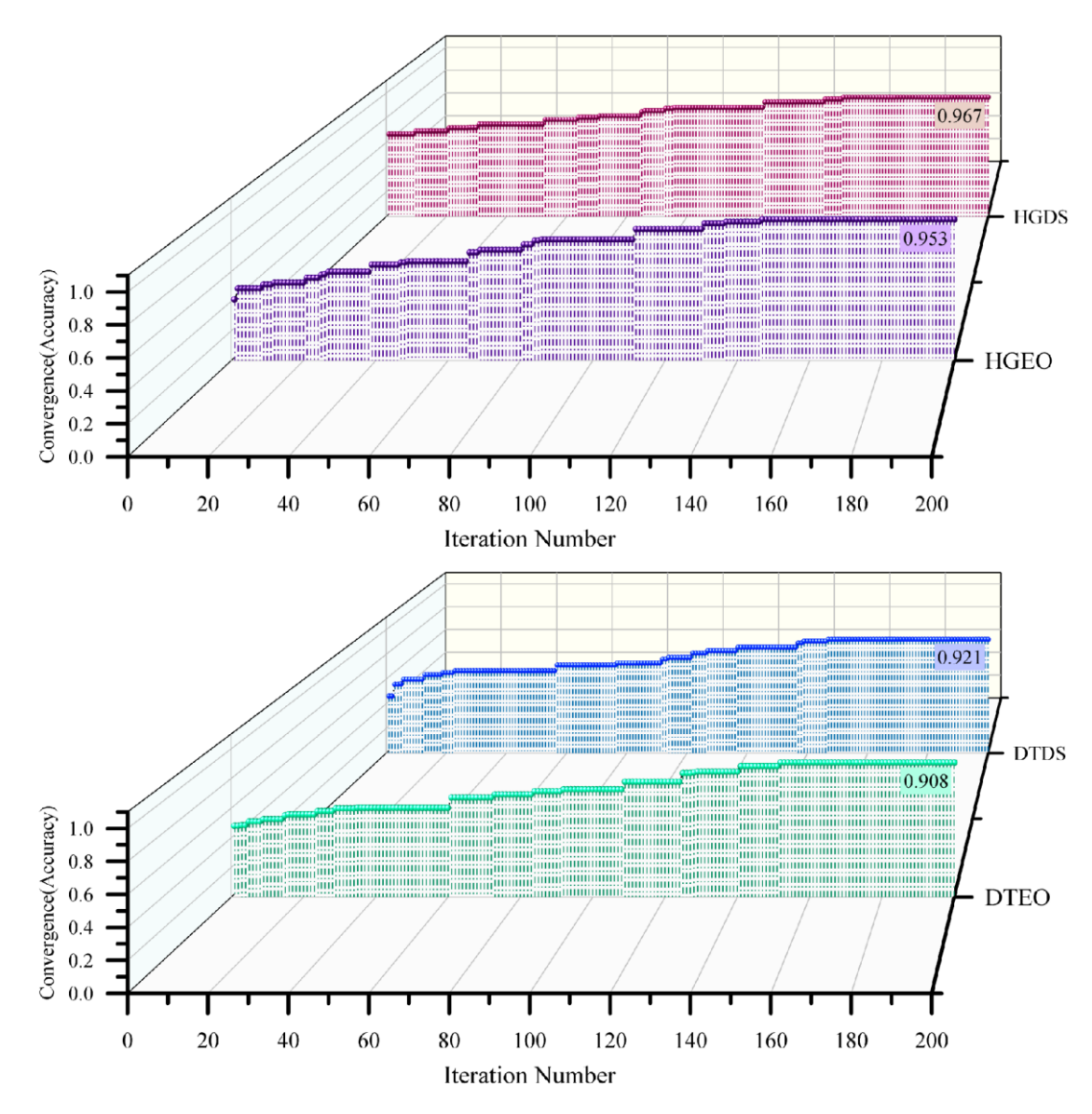
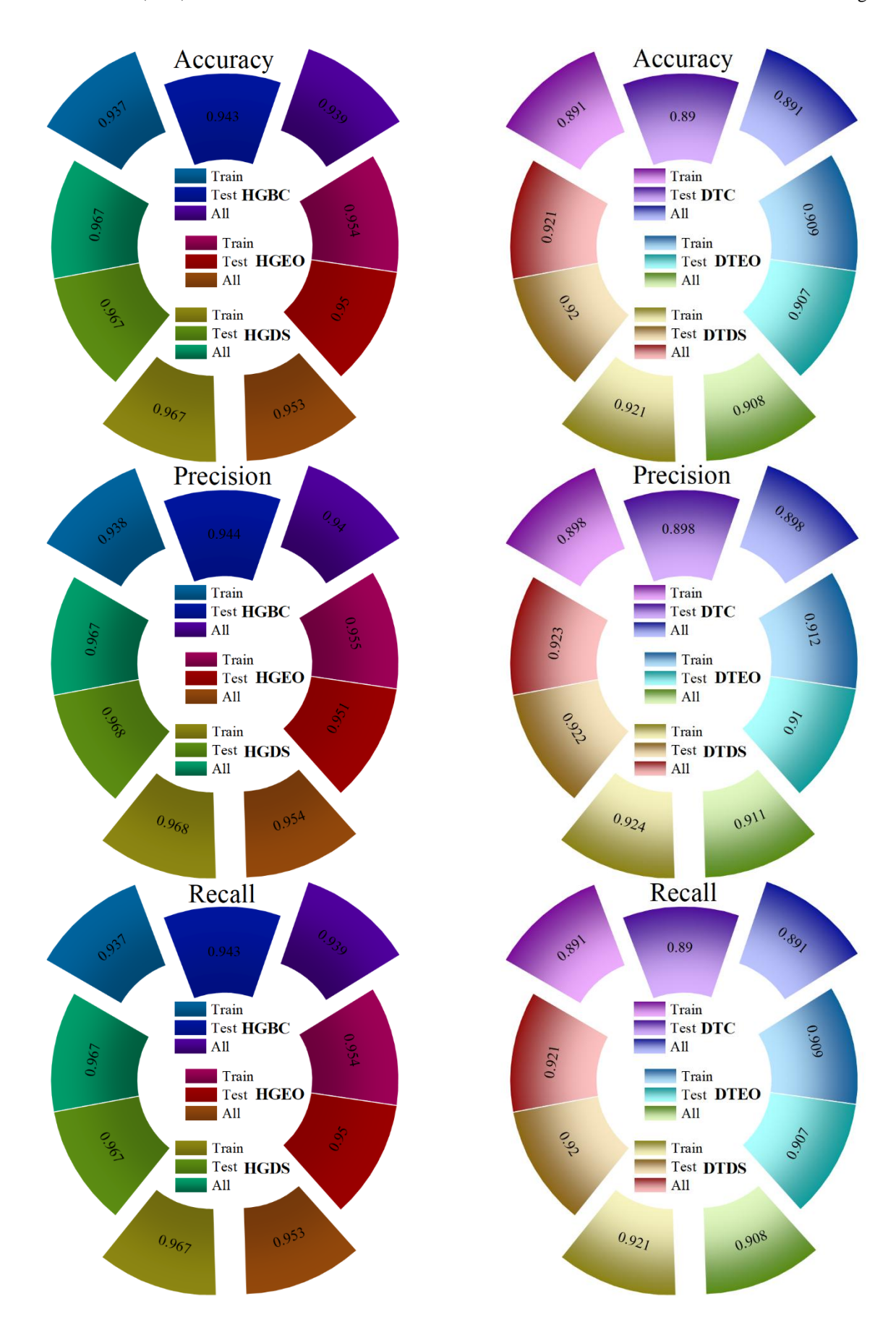


Figure 4: 3D waterfall plot for the convergence curve of the hybrid schemes

3.2 **Schemes performance comparison**

Fig. 5 presents a doughnut plot, providing an intuitive representation of the schemes' performance facilitating a clearer comparison across different evaluation metrics. The performance results of six hybrid schemes evaluated using accuracy, precision, recall, and F1 scores across training, testing, and overall sections have been presented. Among these, HGDS emerges as the best-performing model, with an impressive accuracy of 0.967 in the test section. Conversely, DTEO, with an

accuracy of 0.907, is the weakest model. HGDS outperforms HGEO by 0.17 in accuracy, establishing itself as the top model. Nevertheless, HGEO still demonstrates strong performance, securing the second-best position overall. This comparison underscores the varying strengths of each model, with HGDS leading in accuracy and other performance metrics, while HGEO, despite its lower accuracy, remains a competitive alternative. The results emphasize that even schemes with slightly lower accuracy can still offer valuable performance in certain contexts.



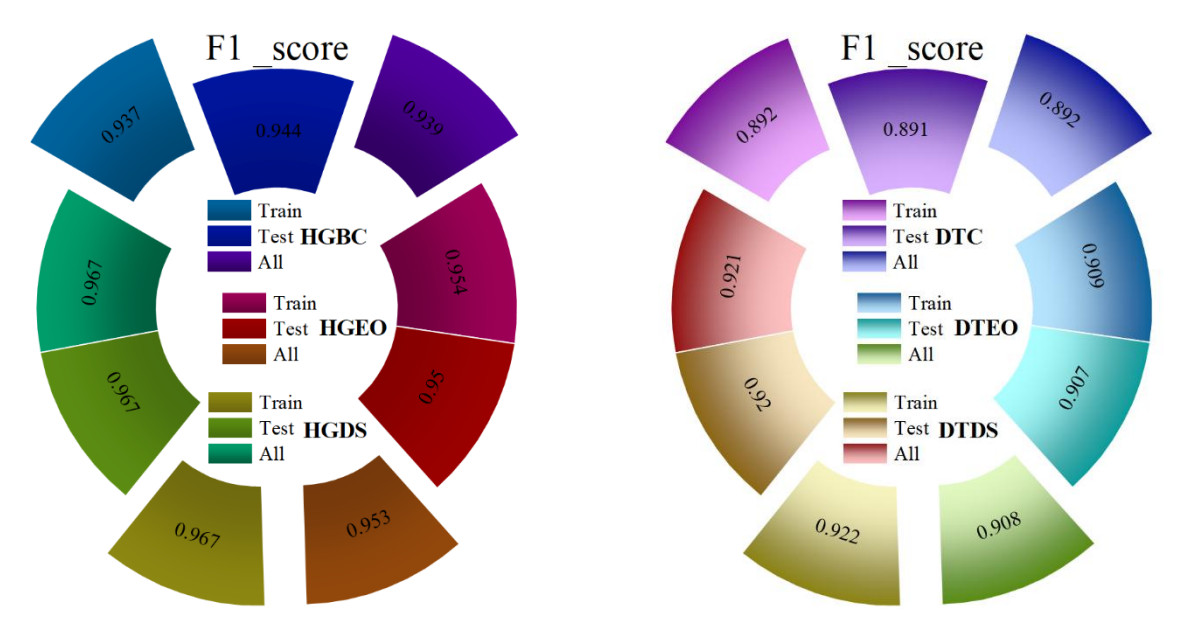


Figure 5: A connected doughnut plot employed for the visual evaluation of the schemes' performance

Additionally, Table 2 provides a summary of the performance of six schemes across five levels regarding precision, recall, and F1 score. The hybrid model HGDS stands out at level 1, achieving the highest precision of 0.990. Additionally, HGDS excels in both recall and F1score, outperforming all other schemes and demonstrating its overall robustness. In contrast, DTEO shows weaker recall performance compared to the other schemes, although it surpasses DTC in this metric. Regarding the F1-score, DTEO records a value of 0.922, which is lower than the top-performing schemes. Nonetheless, it outperforms both DTDS and CTC by margins of 0.013 and 0.010, respectively. While DTEO's F1-score may not be the highest, it still demonstrates competitive performance relative to other schemes. These findings indicate that HGDS is the most well-rounded and effective model overall, while DTEO, despite its limitations in recall and F1 score, delivers superior performance in specific areas.

Immersion Levels Evaluators Schemes Level 1 Level 2 Level 3 Level 4 Level 5 **HGBC** 0.946 0.946 0.909 0.925 0.973 0.995 0.907 0.974 **HGEO** 0.941 0.951 **HGDS** 0.974 0.990 0.981 0.945 0.943 **Precision** DTC 0.988 0.938 0.825 0.909 0.822 **DTEO** 0.973 0.929 0.847 0.923 0.878 **DTDS** 0.906 0.939 0.873 0.914 0.983 **HGBC** 0.951 0.933 0.928 0.952 0.932 0.959 0.947 0.969 **HGEO** 0.946 0.947 **HGDS** 0.960 0.971 0.985 0.956 0.963 Recall DTC 0.847 0.875 0.953 0.869 0.916 **DTEO** 0.876 0.885 0.948 0.927 0.906 **DTDS** 0.911 0.894 0.964 0.927 0.911 0.918 **HGBC** 0.948 0.94 0.938 0.952 0.949 **HGEO** 0.943 0.97 0.932 0.971 **HGDS** 0.975 0.976 0.965 0.949 0.971 F1-score DTC 0.912 0.906 0.885 0.888 0.866 **DTEO** 0.922 0.906 0.895 0.925 0.892 DTDS 0.909 0.916 0.916 0.921 0.946

Table 2: Schemes' evaluation results through different immersion levels

Fig. 6 displays the ROC (Receiver Operating Characteristic) curves of the hybrid model across five immersion levels. The ROC curve plots the True Positive Rate (TPR) against the False Positive Rate (FPR) at various thresholds, offering a visual assessment of the model's ability to distinguish between classes. A higher

Under the Curve (AUC) signifies better performance. Among the five levels, Level 1 has the highest AUC, indicating greater confidence and fewer classification uncertainties at this stage. Conversely, Level 5 shows the weakest ROC performance, likely due to increased data overlap and less feature separation at higher immersion ratings. This suggests that as responses become more subtle at deeper immersion levels, the model's ability to differentiate between classes slightly diminishes, resulting in more false positives and a lower true positive rate. These differences illustrate the model's changing confidence in classification across varying immersion levels. Level 1 is considered the best projection level, characterized by the highest true positive rate and the

lowest false positive rate. At this level, the true positive rate starts at 0.0 and gradually increases to 1.0, while the false positive rate begins at 0.0 and rises to 0.1. On the other hand, Level 5 displays the worst projection performance, with the true positive rate reaching 1.0, indicating a decrease in projection accuracy and an increase in false positive rate. This shows a decline in overall predictive quality as the level increases.

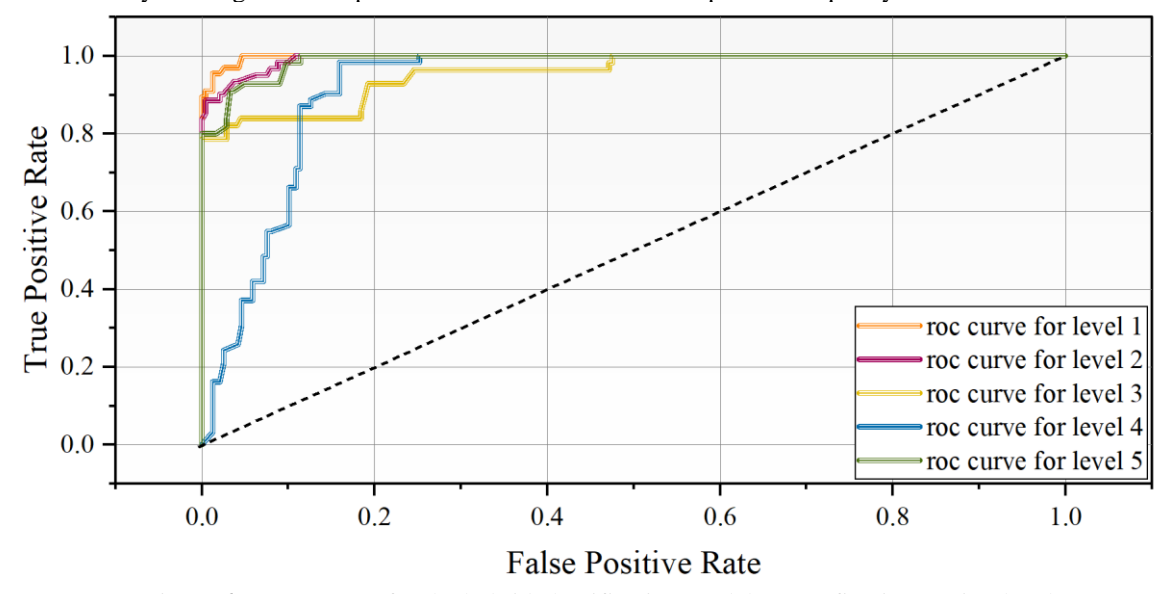


Figure 6: ROC curves for the hybrid classification model across five immersion levels.

3.3 Comparison of the measured and projected values

Fig. 7 displays a 3D bar plot illustrating the correlation between observed and projected values across five levels, highlighting each model's predictive accuracy. Among these, the HGDS model stands out with the best performance, particularly in level 1, where it achieves 194 accurate projections, establishing it as the top-performing

model. This high correlation between observed and projected values underscores HGDS's strong overall reliability. Conversely, the DTEO model shows the weakest performance, with only 177 accurate projections, making it the least effective model overall. While certain schemes may perform poorly in specific conditions, DTEO consistently underperforms across all levels, indicating significant limitations in its predictive accuracy.

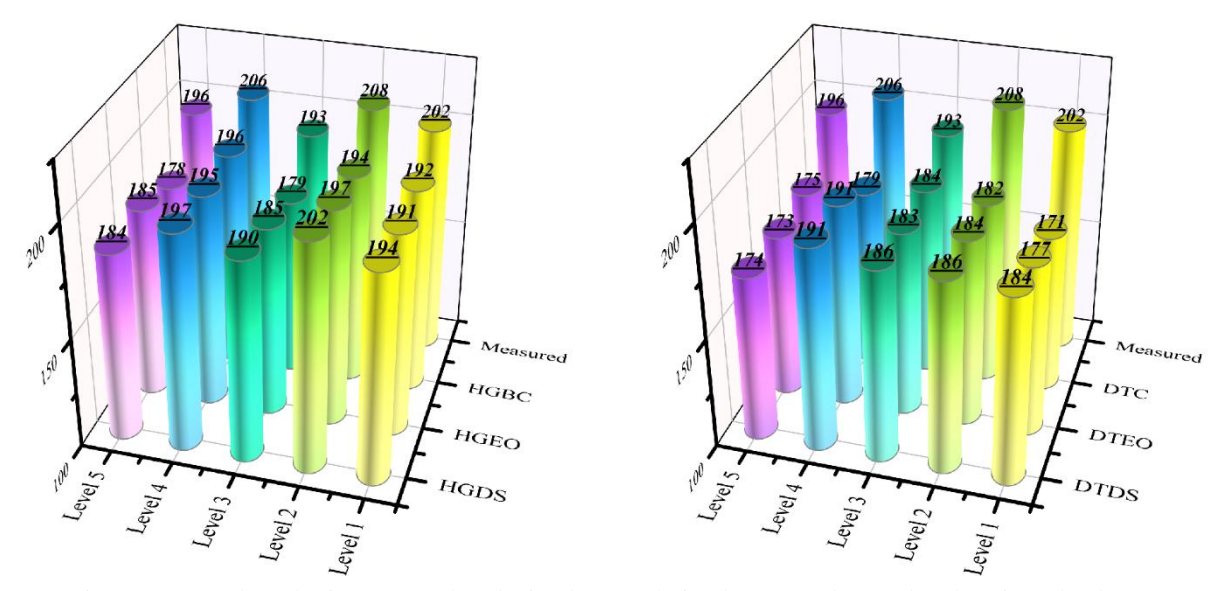


Figure 7: A 3D bar plot is generated to depict the correlation between observed and projected values

Fig. 8 shows the projection errors across six schemes, focusing on correct projections versus mistakes. Among

these, the HGDS stands out for its higher accuracy. In level 1, it correctly projected 192 out of 194 cases,

resulting in only two errors. Similarly, in level 2, HGDS achieved 198 correct projections out of 202, with just four mistakes. This accuracy highlights its strong performance in comparison to the other schemes. In contrast, the DTEO model demonstrates weaker predictive accuracy. In level 1, it recorded five errors out of 177 projections. Its

performance was similarly low in level 2, where it made 14 mistakes out of 184 projections. This high error rate marks DTEO as the least effective among the schemes analyzed. Overall, while HGDS exhibits consistent accuracy in both levels, DTEO's elevated error rate suggests limitations in its predictive reliability.

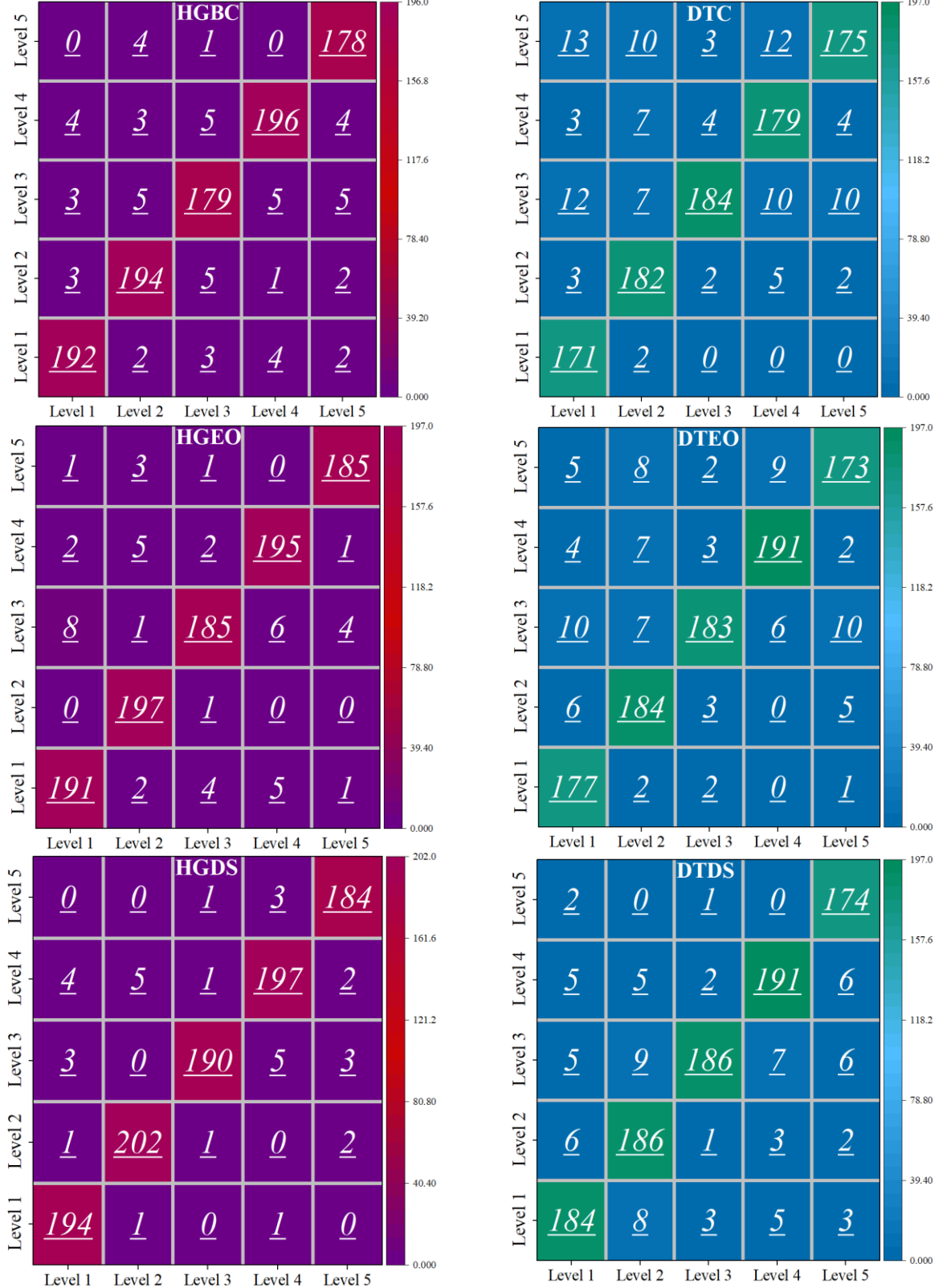


Figure 8: Confusion matrix illustrating the accuracy of the schemes under four specified conditions

• Sensitivity analysis

Table 3 displays the results of a sensitivity analysis using one-way ANOVA to determine if model performance differences across various VR immersion levels are statistically significant. The F-value indicates the ratio of variance between groups to within groups, while the P-value shows the likelihood that observed differences are due to chance. A P-value below 0.05 is generally considered significant. Of the six models evaluated, the DTC model had the highest F-value of 2.923 and a P-value of 0.088. Although close to significance, this result remains statistically non-significant, implying only marginal performance differences that do not meet the 95% confidence threshold.

The HGBC, HGEO, HGDS, DTEO, and DTDS models recorded much lower F-values—0.021, 0.006, 0.031, 1.015, and 0.074—with P-values of 0.886, 0.937, 0.861, 0.314, and 0.786. These findings indicate no statistically significant performance differences across immersion levels. Notably, the HGDS model—identified earlier as the most accurate with a test accuracy of 0.967—showed a low F-value of 0.031 and a high P-value of 0.861, confirming its stable performance across all conditions. Overall, the ANOVA results suggest that none of the models exhibit statistically significant performance variations across immersion levels, highlighting the robustness of the proposed models and particularly validating the consistent performance of HGDS under different experimental scenarios.

Table 3: Sensitivity analysis based on ANOVA

Models name	F-value	P-value	Models name	F-value	P-value
HGBC	0.021	0.886	DTC	2.923	0.088
HGEO	0.006	0.937	DTEO	1.015	0.314
HGDS	0.031	0.861	DTDS	0.074	0.786

3.4 Limitations and directions for future research

While the hybrid classification framework demonstrates encouraging results in predicting VR immersion levels, there are some limitations to address. First, the dataset is relatively small and was collected in a controlled experimental setting, raising questions about how well the models will perform in real-world or commercial VR environments with more diverse users. Second, the computational cost of metaheuristic algorithms like EOS and DSSA can increase substantially with larger dataset dimensions, which may affect real-time or low-latency VR applications. More research is needed to evaluate their scalability and efficiency in live systems. Third, although the models were optimized for accuracy, aspects like interpretability and user feedback were not thoroughly explored. Transparency could be especially important for applications in education or healthcare. Future research will focus on: (1) expanding the dataset to include multimodal user feedback (e.g., eye tracking, EEG), (2) comparing our framework with common models such as SVM, Random Forest, and Neural Networks, and (3) creating lightweight or approximate versions of EOS and DSSA suitable for real-time immersive use. Additionally, we aim to test the models across various VR fields, rehabilitation, including industrial training, personalized learning, to ensure their robustness in different operational contexts.

4 Conclusion

VR simulation immerses users in a dynamic, visually engaging virtual environment where they can navigate, manipulate virtual objects, and interact with digital agents. A defining feature of VR worlds is their three-dimensional nature, often coupled with realistic elements, not only in

their visual representation but also in how objects behave. For instance, VR simulations may include natural forces like gravity. These environments are not always designed to mirror the real world; in fact, they often present fantastical or even impossible scenarios. This unique capability allows VR to simulate complex or hazardous situations safely, making it especially useful in training and educational contexts. In such settings, VR can expose learners to potentially risky situations they might encounter in reality, allowing them to experience and practice without the associated risks. Advancements in technology have greatly enhanced the capabilities of VR, allowing for more immersive and realistic simulations. Additionally, the integration of sophisticated classification schemes, such as DTC and HGBC, is transforming digital experiences. These schemes, along with optimizations from techniques like the EOS and DSSA, contribute to the improvement of VR systems. In testing, the hybrid HGDS approach has proven to be highly effective, achieving an accuracy rate of 0.967, making it the top performer among various schemes. On the other hand, the DTEO approach, with an accuracy of 0.907, was identified as the least effective. Additionally, although this study concentrated on the new EOS and DSSA algorithms because of their innovative hybrid search abilities, future research will include implementing and comparing more traditional and popular optimizers like Particle Swarm Optimization (PSO), Genetic Algorithms (GA), and Bayesian Optimization. This will enable a more comprehensive assessment of optimization efficiency and adaptability across different learning scenarios. Although this study concentrated on hybrid variants within our optimization framework, future research will include benchmarking with models like Random Forest, Support Vector Machines, XGBoost, and Neural Networks. This will contextualize our models' performance against recognized standards and strengthen the validation of our methodology. Despite this, the hybrid approach often outperformed both DTC and DTDS in certain metrics, demonstrating the potential of combining these innovative techniques for enhancing VRbased applications.

Declarations

Funding

This investigation was not funded by any specific grant from public, commercial, or charitable funding bodies.

Authors' contributions

YS performed Data collection, modeling, and appraisal. HZ reviews the initial draft of the manuscript, editing and writing.

Acknowledgements

This exploration was backed by the project of the sixth phase of the "333 High-level Talent Cultivation Project" in Jiangsu Province.

Ethical approval

The exploration has received ethics approval from the IRB, guaranteeing the protection of participants' rights and compliance with the related ethics norms.

References

- C. Anthes, R. J. García-Hernández, [1] Wiedemann, and D. Kranzlmüller, "State of the art of virtual reality technology," in 2016 IEEE aerospace conference, IEEE, Big Sky, MT, USA, pp. https://doi.org/10.1109/AERO.2016.7500674.
- [2] I. Wohlgenannt, A. Simons, and S. Stieglitz, "Virtual reality," Business & Information Systems Engineering, vol. 62, pp. 455-461, 2020. Springer. https://doi.org/10.1007/s12599-020-00658-9.
- J. M. Zheng, K. W. Chan, and I. Gibson, "Virtual [3] reality," Ieee Potentials, vol. 17, no. 2, pp. 20-23, 1998. IEEE. https://doi.org/10.1109/45.666641.
- [4] G. C. Burdea, Virtual reality technology. John Wiley & Sons, 2003.
- S. M. LaValle, Virtual reality. Cambridge [5] university press, 2023.
- [6] R. W. Langacker, "Virtual reality," 1999.
- [7] S. Greengard, Virtual reality. Mit Press, 2019.
- [8] F. P. Brooks, "What's real about virtual reality?" IEEE Computer graphics and applications, vol. no. 6, pp. 16-27, 1999. https://doi.org/10.1109/38.799723.
- [9] M. J. Schuemie, P. Van Der Straaten, M. Krijn, and C. A. P. G. Van Der Mast, "Research on presence in virtual reality: A survey," Cyberpsychology & behavior, vol. 4, no. 2, pp.

- 183-201. 2001. Mary Ann Liebert. https://doi.org/10.1089/109493101300117884.
- W. R. Sherman and A. B. Craig, "Understanding [10] virtual reality," San Francisco, CA: Morgan Kauffman, 2003. Elsevier.
- [11] J. Vince, *Introduction to virtual reality*. Springer Science & Business Media, 2011.
- [12] S. Kavanagh, A. Luxton-Reilly, B. Wuensche, and B. Plimmer, "A systematic review of virtual reality in education," Themes in science and technology education, vol. 10, no. 2, pp. 85-119, 2017. The Learning and Technology Library.
- S. Helsel, "Virtual reality and education," [13] Educational Technology, vol. 32, no. 5, pp. 38-42, 1992.JSTOR.
- [14] W. Winn, "Learning in artificial environments: Embodiment, embeddedness and dynamic adaptation," Technology, Instruction, Cognition and Learning, vol. 1, no. 1, pp. 87–114, 2003.
- B. J. Baker, "Virtual reality," in Encyclopedia of [15] Sport Management, Edward Elgar Publishing, 2024, 1021–1023. Elgar Online. pp. https://doi.org/10.4337/9781035317189.ch599.
- [16] Y. Boas, "Overview of virtual reality technologies," in Interactive Multimedia Conference, 2013, pp. 1-6.
- M.-S. Yoh, "The reality of virtual reality," in [17] Proceedings seventh international conference on virtual systems and multimedia, IEEE, Berkeley, 2001, USA, pp. 666-674. https://doi.org/10.1109/VSMM.2001.969726
- J. S. Bruner, "The act of discovery.," Harvard [18] educational review, 1961. APA PsycNet.
- [19] G. Riva, "Virtual reality," in The Palgrave Encyclopedia of the possible, Springer, 2023, pp. 1740-1750. https://doi.org/10.1007/978-3-030-90913-0 34.
- C. Christou, "Virtual reality in education," in [20] Affective, interactive and cognitive methods for elearning design: creating an optimal education experience, IGI Global, 2010, pp. 228-243. IGI Global. DOI: 10.4018/978-1-60566-940-3.ch012.
- M. Heim, "The design of virtual reality," Body & [21] Society, vol. 1, no. 3-4, pp. 65-77, 1995. Sage Publications. https://doi.org/10.1177/1357034X95001003004.
- R. Dachselt and A. Hübner, "Three-dimensional [22] menus: A survey and taxonomy," Computers & Graphics, vol. 31, no. 1, pp. 53-65, 2007. Elsevier. https://doi.org/10.1016/j.cag.2006.09.006.
- P. Milgram and F. Kishino, "A taxonomy of [23] visual displays," **IEICE** mixed reality TRANSACTIONS on Information and Systems, vol. 77, no. 12, pp. 1321–1329, 1994.
- [24] M. R. Macedonia and M. J. Zyda, "A taxonomy for networked virtual environments," IEEE multimedia, vol. 4, no. 1, pp. 48-56, 1997. IEEE. https://doi.org/10.1109/93.580395.
- [25] A. Mania and A. G. Chalmers, "A classification for user embodiment in collaborative virtual

- environments," in 4th Internatioal Conference on Virtual Systems and Multimedia, Gifu, Japan, 1998.
- [26] D. A. Bowman and L. F. Hodges, "Formalizing the design, evaluation, and application of interaction techniques for immersive virtual environments," *Journal of Visual Languages & Computing*, vol. 10, no. 1, pp. 37–53, 1999. Elsevier. https://doi.org/10.1006/jvlc.1998.0111.
- [27] D. A. Bowman, D. Koller, and L. F. Hodges, "A methodology for the evaluation of travel techniques for immersive virtual environments," *Virtual reality*, vol. 3, no. 2, pp. 120–131, 1998. Springer. https://doi.org/10.1007/BF01417673.
- [28] M. R. Mine, "Virtual environment interaction techniques," *UNC Chapel Hill CS Dept*, 1995.
- [29] J. L. Gabbard, "A taxonomy of usability characteristics in virtual environments," 1997, *Virginia Tech*.
- [30] S. Livatino and C. Koffel, "Handbook for evaluation studies in virtual reality," in 2007 IEEE symposium on virtual environments, human-computer interfaces and measurement systems, IEEE, Ostuni, Italy, 2007, pp. 1–6. https://doi.org/10.1109/VECIMS.2007.4373918.
- [31] G. Welch and E. Foxlin, "Motion tracking: No silver bullet, but a respectable arsenal," *IEEE Computer graphics and Applications*, vol. 22, no. 6, pp. 24–38, 2002.IEEE. https://doi.org/10.1109/MCG.2002.1046626.
- [32] S. Emami and G. Martínez-Muñoz, "Condensed-gradient boosting," *International Journal of Machine Learning and Cybernetics*, pp. 1–15, 2024. Springer. https://doi.org/10.1007/s13042-024-02279-0.
- [33] F. Pedregosa *et al.*, "scikit-learn: Machine Learning in Python-StandardScaler, 2011," 2024, *Accessed*.
- [34] F. T. Admojo and B. S. W. Poetro, "Comparative Study on the Performance of the Bagging Algorithm in the Breast Cancer Dataset," *International Journal of Artificial Intelligence in Medical Issues*, vol. 1, no. 1, pp. 36–44, 2023. Yoctobrain.
 - https://doi.org/10.56705/ijaimi.v1i1.87.
- [35] A. Naswin and A. P. Wibowo, "Performance Analysis of the Decision Tree Classification Algorithm on the Pneumonia Dataset," *International Journal of Artificial Intelligence in Medical Issues*, vol. 1, no. 1, pp. 1–9, 2023. https://doi.org/10.56705/ijaimi.v1i1.83.
- [36] T. I. A. Mohamed, O. N. Oyelade, and A. E. Ezugwu, "Automatic detection and classification of lung cancer CT scans based on deep learning and ebola optimization search algorithm," *Plos one*, vol. 18, no. 8, p. e0285796, 2023. PLOS. https://doi.org/10.1371/journal.pone.0285796.